



HAL
open science

Monte Carlo simulation of a scintillation crystal read by a SiPM with GATE

Brahim Mehadji, Mathieu Dupont, Denis Fougeron, Christian Morel

► To cite this version:

Brahim Mehadji, Mathieu Dupont, Denis Fougeron, Christian Morel. Monte Carlo simulation of a scintillation crystal read by a SiPM with GATE. 9th Conference on New Developments in Photodetection, Jul 2022, Troyes, France. pp.167905, 10.1016/j.nima.2022.167905 . hal-03910499

HAL Id: hal-03910499

<https://hal.science/hal-03910499v1>

Submitted on 5 Apr 2023

HAL is a multi-disciplinary open access archive for the deposit and dissemination of scientific research documents, whether they are published or not. The documents may come from teaching and research institutions in France or abroad, or from public or private research centers.

L'archive ouverte pluridisciplinaire **HAL**, est destinée au dépôt et à la diffusion de documents scientifiques de niveau recherche, publiés ou non, émanant des établissements d'enseignement et de recherche français ou étrangers, des laboratoires publics ou privés.

Monte Carlo simulation of a scintillation crystal read by a SiPM with GATE

Brahim Mehadji^{a,b}, Mathieu Dupont^a, Denis Fougeron^a, and Christian Morel^a

^a*Aix-Marseille Univ, CNRS/IN2P3, CPPM, Marseille, France*

^b*present address: Aix Marseille Univ, APHM, Hôpital de la Timone et Nord, Médecine Nucléaire, Marseille, France*

Abstract

Silicon photomultipliers (SiPMs) have recently emerged as a replacement for photomultiplier tubes (PMTs) for light detection in many applications, including high-energy physics and medical imaging. Recently, detailed Monte Carlo simulation of SiPMs has been implemented in GATE to quantify the impact of SiPM specifications on the linearity, energy and time resolution of a scintillation crystal read by a SiPM. In this paper, GATE simulations of a LYSO crystal coupled to a SiPM are compared to measurements. The energy spectra of the ²⁴¹Am and ²²Na radioactive sources are found to agree with less than 2% difference. The linearity of the SiPM response is duly affected by the SiPM saturation and, as seen above 511 keV with our configuration, it is slightly enhanced by the generation of crosstalk. Furthermore, with an over-voltage close to that recommended by the manufacturer, all sources of SiPM noise contribute about equally to the degradation of the energy resolution at low energies, which is downgraded by more than 15% at 60 keV, but have less impact at higher energies. In addition, the GATE simulations show that crosstalk plays an important role on the time resolution of the installation.

Keywords: Monte Carlo simulation, GATE, SiPM, CTR, gamma-ray spectrometry.

1. Introduction

Silicon photomultipliers (SiPMs) replace photomultiplier tubes (PMTs) for light detection in many applications, including high-energy physics and medical imaging [1] [2] [3]. SiPMs are composed of thousands of micro avalanche photodiodes [4]. Their sizes vary from one to tens of millimeters depending on the SiPM model. The detection of an optical photon by one micro avalanche photodiode (also called micro-cell) induces an electric signal (pulse), which approximately follows a double exponential decay. The sum of all the pulses issued by the micro-cells gives the SiPM signal, which is very sensitive to temperature and over-voltage [5]. Various sources of correlated noise — crosstalks (micro-cells that fire due to infrared excitation resulting from the avalanche of another neighbor micro-cell), after-pulses (a micro-cell that fires again a few nanoseconds after the bulk interaction resulting from a first avalanche within the micro-cell), delayed-crosstalks (a micro-cell that fires a few nanoseconds after the bulk interaction resulting from a first avalanche in another micro-cell) — and uncorrelated noise — dark counts (a random firing of a micro-cell due to thermic excitation) and white noise — perturb this signal.

Email address: mehadji@cppm.in2p3.fr (Brahim Mehadji)

14 Recently, detailed simulation of analog SiPMs has been implemented in GATE [6] [7] to quantify the
 15 impact of SiPM specifications on the linearity, energy and temporal resolution of a scintillation crystal read
 16 by a SiPM.

17 In this paper, GATE simulations of a LYSO crystal coupled to a SiPM or to a PMT are compared
 18 to measurements. The comparison between the simulated and measured PMT energy spectra (i.e., in the
 19 absence of significant sources of correlated and uncorrelated noise) of ^{241}Am and ^{22}Na radioactive sources is
 20 used to normalize the SiPM data for the intrinsic linearity and resolution of the LYSO scintillation response.
 21 This allows the non-linearity of the SiPM response due to its limited number of cells to be assessed on
 22 the simulated data and the impact of SiPM noise on energy and time resolution to be quantified using an
 23 over-voltage close to that recommended by the manufacturer.

24 2. Measured and simulated data of a LYSO crystal read by a PMT

25 The experimental setup consists of a polished $3 \times 3 \times 5 \text{ mm}^3$ scintillating crystal of lutetium-yttrium
 26 oxyorthosilicate (LYSO) from Crystal Photonics. The unwrapped crystal was positioned without optical
 27 coupling on the photocathode surface of a PMT 9125WB (11 dynodes, photon detection efficiency (PDE)
 28 @ 420 nm: 28%, single electron resolution (SER): 7.5 ns FWHM) from ET Enterprises, connected to an
 29 oscilloscope HDO9404-MS from LeCroy. The crystal was irradiated with 60, 511 and 1275 keV gamma
 30 rays emitted by ^{241}Am and ^{22}Na radioactive sources.

31 2.1. Photo-peak measurements

32 The PMT signals were integrated and results were plotted in histograms to get energy spectra. Figure 2
 33 shows the measured photo-peaks at 60, 511 and 1275 keV. Photo-peak positions and resolutions (FWHM)
 34 result from fitting a Gaussian superimposed on a linear background. Photo-peak positions show a non
 35 linearity of 18% of the LYSO scintillation response at 60 keV compared to 511 keV, while it is negligible
 36 ($< 1\%$) at 1275 keV [8]. These values will be used to set the scintillation light yield of LYSO at 60, 511 and
 37 1275 keV in GATE.

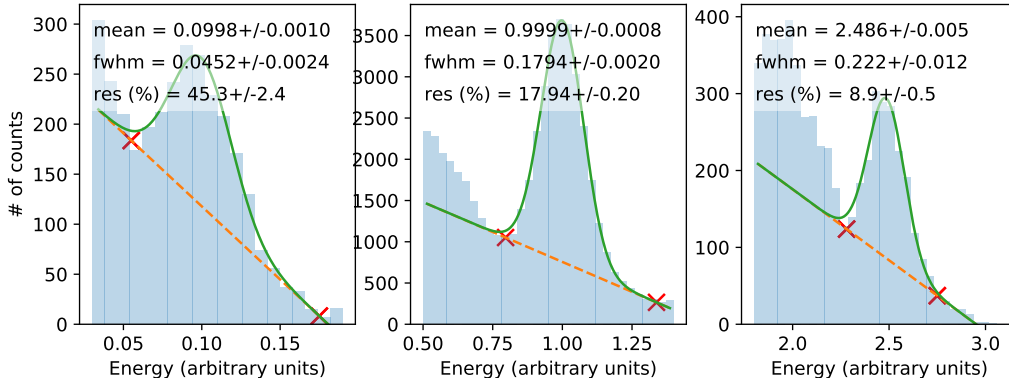


Fig. 1. Measured energy spectra for a $3 \times 3 \times 5 \text{ mm}^3$ LYSO crystal read by a PMT for incident gamma rays of (left) 60 keV, (center) 511 keV and (right) 1275 keV. Energy scale (in arbitrary units) is normalized to the 511 keV photo-peak position. The peak positions and resolutions result from fitting (in green) a Gaussian superimposed on a linear background.

38 2.2. GATE simulations

39 To model our experimental setup with GATE, the PDE of the PMT and the crystal composition ($\text{Lu}_{1.8}\text{Y}_{0.2}\text{Si}_{1.0}\text{O}_{5.0}$),
 40 density (7.05 g/cm^3), refractive index (1.81), and scintillation light yield ($LY = 28\,000 \text{ ph/MeV}$) and fall-off
 41 decay time ($\tau_d = 42 \text{ ns}$) were instantiated from specifications provided in the literature [9] and by the man-
 42 ufacturers. The scintillation rise time constant was set to 57 ps with a resolution of 20 ps FWHM according

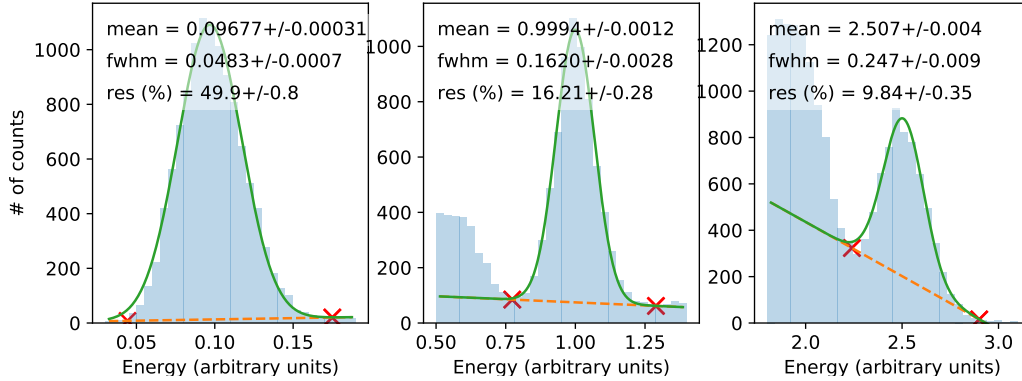


Fig. 2. Simulated energy spectra for a $3 \times 3 \times 5 \text{ mm}^3$ LYSO crystal read by a PMT for incident gamma rays of (left) 60 keV, (center) 511 keV and (right) 1275 keV. Energy scale (in arbitrary units) is normalized to the 511 keV photo-peak position. The peak positions and resolutions result from fitting (in green) a Gaussian superimposed on a linear background.

43 to [10]. The non linearity of scintillation response of the crystal was set according to the measurements
 44 described in the previous section. Finally, we used the *Rought_LuT* surface type from the University of
 45 California Davis Look Up Table [11] [12].

46 In GATE, the number of scintillation photons generated for an energy E deposited in the crystal is
 47 distributed with a Gaussian of mean $E \times LY$ and standard deviation $RESOLUTIONSCALE \times \sqrt{E \times LY}$.
 48 The parameter *RESOLUTIONSCALE* accounts for the impact of the non-linearity of the light yield at
 49 low energy, which degrades energy resolution because of the balance between photoelectric interaction and
 50 Compton scattering while collecting the total energy deposit in the crystal that results from the sum of con-
 51 tributions at different energies [8]. Once set to 4.41, the parameter *RESOLUTIONSCALE* is reproducing
 52 at best the measured energy resolutions.

53 2.3. Comparison of measured and simulated data of a LYSO crystal read by a PMT

54 Table 1 lists the measured and simulated photo-peak resolutions (FWHM) for incident gamma rays of
 55 60, 511 and 1275 keV. Despite the adjustment of the scintillation light yields from the measured photo-peak
 56 positions, significant differences are still observed between the simulated and measured energy resolutions
 57 that are probably due to the large intrinsic resolution contribution of the scintillation crystal [13], which is
 58 not taken into account by GATE.

E (keV)	Measured res. (%)	Simulated res. (%)	Relative diff. (%)
60	45.3 ± 2.4	49.9 ± 0.8	10.2 ± 5.6
511	17.9 ± 0.2	16.2 ± 0.4	-9.5 ± 2.2
1275	8.9 ± 0.5	9.8 ± 0.4	10.1 ± 7.19

Table 1. Comparison of the measured and simulated photo-peak resolutions (FWHM) for 60, 511 and 1275 keV gamma rays falling on a LYSO crystal read by a PMT.

59 3. Measured and simulated data of a LYSO crystal read by a SiPM

60 We used here the same experimental setup as in Section 2, except that the PMT was replaced by a
 61 $3 \times 3 \text{ mm}^2$ SiPM MPPC S13360-3050CS (micro-cell pitch: $50 \mu\text{m}$, # cells: 3558, PDE @ 420 nm: 40%,
 62 gain @ $V_{ov} = 3 \text{ V}$: 1.7×10^6 , recovery time: 28.5 ns [6], crosstalk probability: 5.4% [6]) from Hamamatsu
 63 Photonics powered with an over-voltage of 3 V with the C12332-01 card, which contains an OPA846 signal
 64 amplifier from Texas Instrument. The SiPM was coupled to the crystal with an optical grease from Saint-
 65 Gobain with a refractive index of 1.51 and operated at a room temperature of 21 °C.

66 *3.1. Photo-peak measurements*

67 The amplifier was deactivated for measurements at 511 keV and 1275 keV, because otherwise the signal
 68 amplitude saturates. The SiPM signal were numerically integrated during 400 ns with a sampling frequency
 69 of 5 GHz and results were binned in histograms to get energy spectra. Figure 4 (top row) presents the photo-
 70 peaks measured at 60, 511 and 1275 keV. Photo-peak positions and resolutions (FWHM) result from fitting
 71 a Gaussian superimposed on a linear background.

72 *3.2. GATE simulations*

73 We used the same values for the specifications of the LYSO crystal as in Section 2.2. All the parameters
 74 used for the Monte Carlo simulation of the SiPM with GATE are instantiated in the files SiPM.XML and
 75 Surface.XML, which are described in [6]. The SiPM equivalent circuit has a cell capacitance $C_p = 84.5$ pf,
 76 a cell parasitic capacitance $C_q = 16.8$ pF, a SiPM grid capacitance $C_g = 16.8$ pF and a cell quenching
 77 resistance $R_q = 300$ k Ω , but we do not simulate it to generate the SiPM signal in GATE. Instead, the pulse
 78 amplitude and shape of a micro-cell stored in the file SiPM.XML corresponds to the average pulse obtained
 79 by illuminating the entire surface of the SiPM with a 20 ps FWHM laser pulse divided by the number of
 80 micro-cells (3558). Figure 3 presents the measured (blue curve) and simulated (orange curve) mean shapes
 81 and dispersions of SiPM signals for 60, 511 and 1275 keV incident gamma rays.

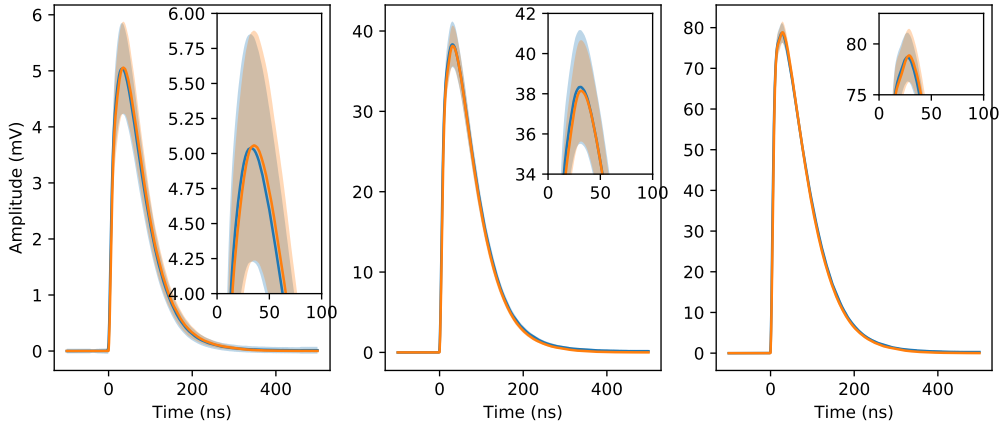


Fig. 3. Measured (blue curve) and simulated (orange curve) mean shapes and dispersions of SiPM signals for (left) 60 keV, (center) 511 keV, and (right) 1275 keV gamma rays falling on a LYSO crystal read by a SiPM.

82 *3.3. Comparison of measured and simulated data of a LYSO crystal read by a SiPM*

83 Measured and simulated energy spectra are compared in Figure 4. Note that for 511 keV gamma rays,
 84 the peak-to-valley depth is smaller for measured data than for simulated data because measurements were
 85 performed using a ^{22}Na radioactive source, which implies a Compton background from the 1275 keV gamma
 86 rays below the 511 keV photo-peak. Nevertheless, the non linearity of SiPM due to the limited number of
 87 micro-cells [14] is correctly simulated by GATE as shown in Figure 5 (left). The non-linearity of SiPM
 88 has a major contribution to the energy resolution since it improves faster with energy than it would with
 89 a linear response. In fact, following [14], the non linear response of SiPM can be modeled by $V(E) =$
 90 $A \times (1 - \exp(-E/(N_{\text{cells}} \times B)))$ where E is the energy and A and B are free parameters. A linear response of
 91 the SiPM $V_{\text{lin}}(E)$ corresponding to the first-order approximation of $V(E)$ can then be estimated by $V_{\text{lin}}(E) =$
 92 $-A \times \ln(1 - V(E)/A)$, which leads to $\Delta V/V = \Delta V_{\text{lin}}/(A \times (\exp(V_{\text{lin}}/A) - 1)) < \Delta V_{\text{lin}}/V_{\text{lin}}$.

93 The photo-peak resolutions of measured and simulated data differ by about 10% for gamma rays of
 94 60 and 511 keV. Indeed, as we noted in Section 2.3, the simulated resolutions do not take into account

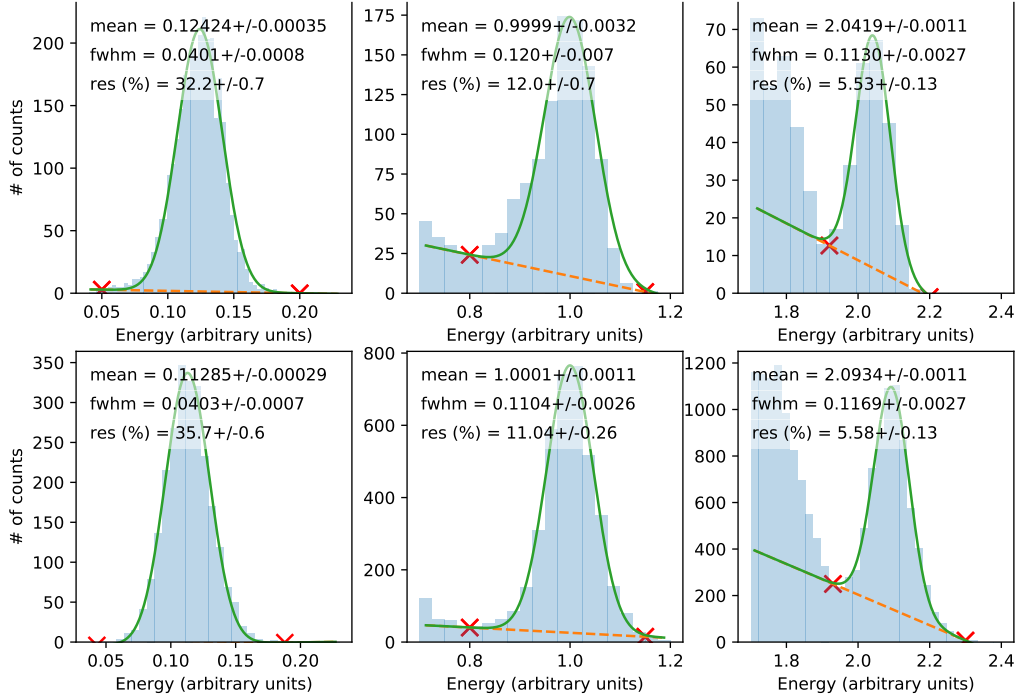


Fig. 4. Measured (top row) and simulated (bottom row) energy spectra for a $3 \times 3 \times 5 \text{ mm}^3$ LYSO crystal read by a SiPM for incident gamma rays of (left) 60 keV, (middle) 511 keV, (right) 1275 keV. Energy scale (in arbitrary units) is normalized to the 511 keV photo-peak position. The peak positions and resolutions result from fitting (in green) a Gaussian superimposed on a linear background.

the intrinsic resolution of the scintillation crystal. For a fair comparison of the measured and simulated SiPM resolutions, we need to normalize the simulated SiPM resolutions by the ratio of the measured and simulated PMT resolutions. However, as the PMT energy spectra are not subject to saturation effects, this normalization requires first correcting the SiPM spectra for the SiPM non-linearity as proposed in [14] (see Figure 5 (right)). Table 2 shows the positions and resolutions (FWHM) of the measured and simulated photo-peaks. A good agreement of less than 1.5% is obtained between the measured and simulated resolutions.

E (keV)	Measurements		Simulations		Relative diff. (%)	
	pos.	res. (%)	pos.	res. (%)	pos.	res.
60	0.11	32.6 ± 0.7	0.11	32.9 ± 0.5	0	0.9
511	1.00	13.5 ± 0.8	1.00	13.3 ± 0.3	0	1.5
1275	2.48	8.6 ± 0.6	2.49	8.5 ± 0.7	0.4	1.2

Table 2. Comparison of the measured and simulated photo-peak positions (in arbitrary units normalized to the 511 keV photo-peak position) and resolutions (FWHM) for incident gamma rays of 60, 511 and 1275 keV after correction of the SiPM non-linearity and normalization of the resolutions by the ratio of the measured and simulated PMT resolutions.

3.4. Impact of SiPM noise sources on energy resolution

In order to determine the effect of the various SiPM noise sources (dark counts, after-pulses and cross-talks) on the energy spectra, simulation studies were carried out with all noise sources disabled or with only one noise source disabled at a time. Table 3 lists the photo-peak positions and resolutions (FWHM) resulting from this study. A significant impact of SiPM noise is observed on the photo-peak resolution for incident gamma rays of 60 keV: disabling the SiPM noise improves the resolution by 15%. A moderate contribution

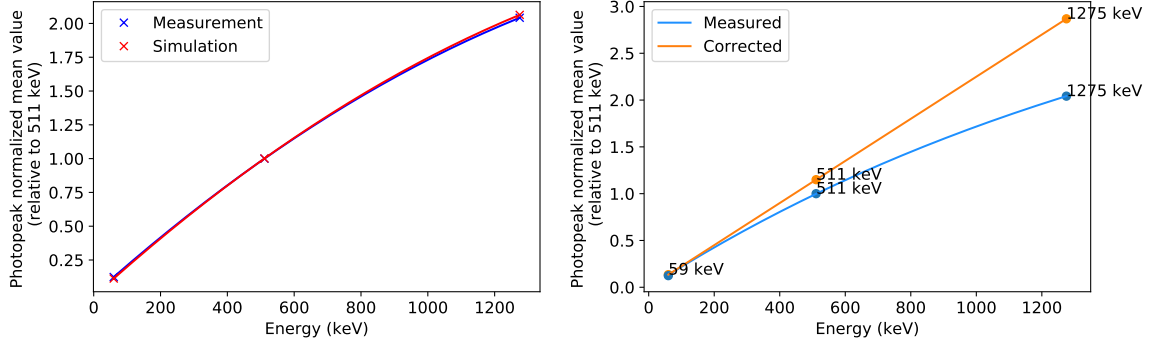


Fig. 5. (left) Comparison of SiPM measured (blue) and simulated (red) photo-peak positions (in arbitrary units normalized to the 511 keV photo-peak position) as a function of the incident gamma ray energy. (right) Correction of the non-linearity of the SiPM energy spectra as proposed in [14].

107 from the SiPM non-linearity can also be seen for the incident gamma rays of 1275 keV: disabling the SiPM
 108 noise increases the position of the photo peak by 2.5%.

E (keV)	With noise		No after-pulses		No crosstalks		No dark counts		No noise	
	pos.	res. (%)	pos.	res. (%)	pos.	res. (%)	pos.	res. (%)	pos.	res. (%)
60	0.11	32.4 ± 0.5	0.11	28.4 ± 1.2	0.11	28.7 ± 0.9	0.11	28.4 ± 1.2	0.11	27.7 ± 1.2
511	1.00	11.0 ± 0.3	1.00	10.9 ± 0.6	1.00	10.2 ± 0.6	1.00	10.3 ± 0.6	1.00	10.3 ± 0.5
1275	2.09	5.6 ± 0.1	2.10	5.3 ± 0.4	2.13	5.3 ± 0.3	2.09	5.5 ± 0.3	2.14	5.2 ± 0.6

Table 3. Simulated photo-peak positions (in arbitrary units normalized to the 511 keV photo-peak position) and resolutions (FWHM) for incident gamma rays of 60, 511 and 1275 keV.

109 Figure 6 displays the average signal shapes obtained by disabling all or only one SiPM noise source at
 110 a time. The average signal amplitude decreases when no noise is simulated. At 3 V over-voltage, crosstalk
 111 makes the largest contribution to the signal, while dark counts make the least.

112 3.5. Measured and simulated coincidence time resolutions (CTR)

113 Simulation of the SiPM time resolution is evaluated by comparing the measured and simulated coinci-
 114 dence time resolutions (CTR) for the detection of 511 keV annihilation pairs by two $3 \times 3 \times 5$ mm³ LYSO
 115 crystals coupled to SiPMs with optical grease and wrapped in Teflon. Each SiPM was connected to an
 116 amplification circuit optimized for timing applications as described in [15]. A ⁶⁸Ge source was placed be-
 117 tween the two detectors and the oscilloscope was set to trigger coincidentally with a threshold level three
 118 times above the electric noise. The time difference between the two signals was plotted in a histogram and
 119 the CTR (FWHM) was estimated using the NEMA protocol [16]. Coincidence time measurements were
 120 performed for several SiPM over-voltages from 4 to 9 V.

121 The method proposed by Rosaldo and Hidalgo [17], which was used in [6] to evaluate the paramaters
 122 necessary to simulated the SiPM noise sources, i.e., ϵ_c (the probability to have at least one crosstalk), C_{AP}
 123 (the probability that an after-pulse occurs at $t = 0$), C_{CT} (a constant expressed in unit of [time]^{-1/2} involved
 124 in the probability of having a delayed-crosstalk) and DCR (dark count rate), cannot be used to simulate the
 125 SiPM operating at high over-voltages. Instead, these four parameters can be extrapolated from measure-
 126 ments obtained with lower over-voltages (below 5 V) using the following equations:

$$\epsilon_c = 1 - e^{-\left(\frac{V_{ov}}{k}\right)^{1+\alpha}} \quad AP = \left(\frac{V_{ov}}{k_{AP}}\right)^{1+\beta}$$

127 where AP stands for either C_{AP} , C_{CT} or DCR, and k , α , k_{AP} and β are fitting parameters. Also note that the
 128 PDE is over-voltage dependent and must be instantiated in GATE using the manufacturer's specifications.

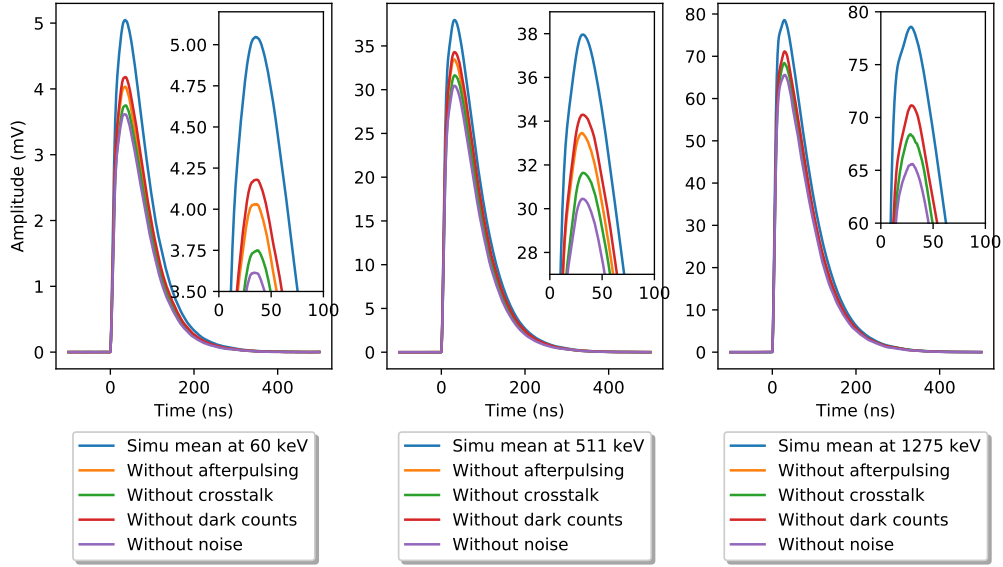


Fig. 6. Average signal shapes obtained by removing all or one SiPM noise source at a time for incident gamma rays of (left) 60 keV, (center) 511 keV and (right) 1275 keV.

129 Finally, we used the *Rough.Teflon* surface type of the UNIFIED model [18] with a reflectivity of 52%
 130 to describe the crystal surfaces as in [11]. Figure 7 (left) shows the comparison of histograms of measured and simulated coincidence time differences at an over-voltage of 9 V. The measured and simulated CTR as
 131 a function of SiPM over-voltage presented in Figure 7 (right) are in good agreement.
 132

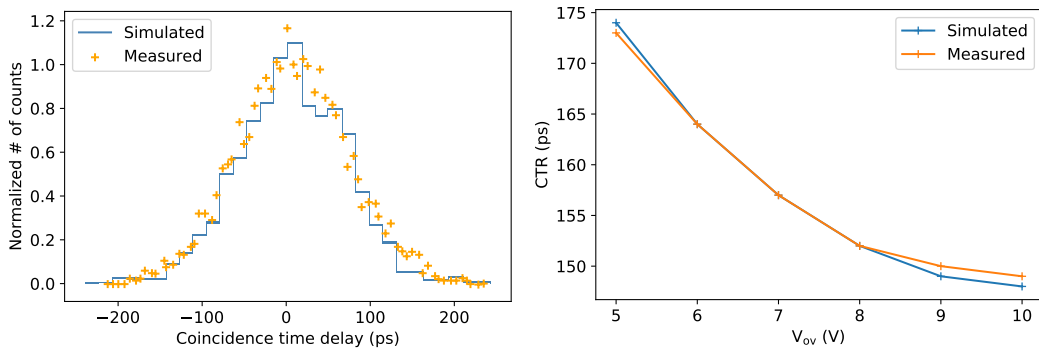


Fig. 7. (left) Comparison of histograms of measured (crosses) and simulated (continuous line) coincidence time differences at an over-voltage of 9 V. (right) Measured and simulated CTR as a function of SiPM over-voltage.

133 3.6. Impact of SiPM noise on CTR

134 To understand the contribution of crosstalk on CTR, a simulation was performed without crosstalk with a
 135 SiPM over-voltage of 9 V. A degradation of CTR of about 4% due to crosstalk is observed. This contribution
 136 increases with over-voltage since crosstalk increases with over-voltage [19]. For instance, Stefan Gundacker
 137 et al., showed in [10] that the impact of the crosstalk on CTR becomes significant above $\epsilon_c = 0.65$.

138 The dependence of CTR as a function of delayed-crosstalks and afterpulses is not studied here since
 139 these latter appear after the SiPM response to detected optical photons. As far as the DCR is concerned, its
 140 contribution is less intuitive. When a dark count appears shortly before the detection of a gamma ray, the

141 estimated time of triggering will be that of the dark count. The time distribution of the DCR being uniform,
142 it will add uniform noise to the CTR. However, if the DCR is very large, it is no longer possible to keep the
143 threshold close to the electrical noise. In this case, the measured CTR will also be impacted.

144 4. Conclusion

145 GATE simulations of a scintillation crystal read by a SiPM were compared successfully to measure-
146 ments. The energy spectra of the ^{241}Am and ^{22}Na radioactive sources for a $3 \times 3 \times 5 \text{ mm}^3$ LYSO crystal
147 coupled to a $3 \times 3 \text{ mm}^2$ SiPM MPPC S13360-3050CS are in agreement with less than 2% difference, and
148 CTRs estimated as a function of the SiPM over-voltage are in good agreement between measurements and
149 simulations.

150 In a second step, the simulations were used to quantify the impact of SiPM noise sources on the en-
151 ergy and time resolutions. With an over-voltage close to that recommended by the manufacturer, all SiPM
152 noise sources contribute about equally to the degradation of the energy resolution at low energies, which
153 is degraded by more than 15% at 60 keV, but have less impact at higher energies. In addition, the GATE
154 simulations show that crosstalk plays an important role on the time resolution of the setup.

155 Acknowledgements

156 *This work was supported by the project TEMPORAL funded by the ANDRA/PIA under the grant No.*
157 *RTSCNADAA160019.*

158 References

- 159 [1] T. Lewellen, Recent developments in PET detector technology, *Phys. Med. Biol.* 53 (2008) R287–317.
- 160 [2] M. Conti, B. Bendriem, The new opportunities for high time resolution clinical TOF PET, *Clin. Transl. Imaging* 7 (2019) 139–147.
- 161 [3] V. Kovaltchouk, et al., Comparison of a silicon photomultiplier to a traditional vacuum photomultiplier, *Nucl. Instrum. Meth. A*
162 538 (2005) 408–415.
- 163 [4] D. Renker, E. Lorenz, Advances in solid state photon detectors, *J. Instrum.* 4 (2009) P04004.
- 164 [5] O. Adam Nepomuk, et al., Characterization of Three High Efficiency and Blue Sensitive Silicon Photomultipliers, *Nucl. Instrum.*
165 *Meth. A* 846 (2017) 106–125.
- 166 [6] B. Mehadji, et al., Monte Carlo simulation of SiPMs with GATE, *J. Instrum.* 17 (2022) P09025.
- 167 [7] D. Sarrut, et al., Advanced Monte Carlo simulations of emission tomography imaging systems with GATE, *Phys. Med. Biol.* 66
168 (2021) 10TR03.
- 169 [8] P. Lecoq, Development of new scintillators for medical applications, *Nucl. Instrum. Meth. A* 809 (2016) 130–139.
- 170 [9] Y. Liu, et al., Performance analysis of LYSO–SiPM detection module for X-ray communication during spacecraft reentry black-
171 out, *Nucl. Instrum. Meth. A* 1013 (2021) 165673.
- 172 [10] S. Gundacker, et al., State of the art timing in TOF-PET detectors with LuAG, GAGG and L(Y)SO scintillators of various sizes
173 coupled to FBK-SiPMs, *J. Instrum.* 11 (2016) P08008.
- 174 [11] M. Stockhoff, et al., Advanced optical simulation of scintillation detectors in GATE V8.0: first implementation of a reflectance
175 model based on measured data, *Phys. Med. Biol.* 62 (2017) L1–L8.
- 176 [12] E. Roncali, et al., An integrated model of scintillator-reflector properties for advanced simulations of optical transport, *Phys.*
177 *Med. Biol.* 62 (2017) 4811–4830.
- 178 [13] C. Dujardin, Inorganic scintillating materials, in *Électronique, photonique, optique photonique*, Tech. rep., Techniques de
179 l'ingénieur, Saint-Denis, France. (2018) EE6347 V1.
- 180 [14] J. Pulko, et al., A monte-carlo model of a SiPM coupled to a scintillating crystal, *J. Instrum.* 7 (2012) P02009.
- 181 [15] S. Gundacker, et al., High-frequency SiPM readout advances measured coincidence time resolution limits in TOF-PET, *Phys.*
182 *Med. Biol.* 64 (2019) 055012.
- 183 [16] NEMA, Performance Measurements of Positron Emission Tomographs (PET) (2018).
- 184 [17] J. Rosado, S. Hidalgo, Characterization and modeling of crosstalk and afterpulsing in Hamamatsu silicon photomultipliers, *J.*
185 *Instrum.* 10 (2015) P10031.
- 186 [18] M. Janecek, W. W. Moses, Simulating Scintillator Light Collection Using Measured Optical Reflectance, *IEEE Trans. Nucl. Sci.*
187 57 (2010) 964–970.
- 188 [19] F. Acerbi, S. Gundacker, Understanding and simulating SiPMs, *Nucl. Instrum. Meth. A* 926 (2019) 16–35.